Nanomed. J. 7(3): 211-224, Summer2020

RESEARCH PAPER

Using 5-fluorouracil-encored plga nanoparticles for the treatment of colorectal cancer: the in-vitro characterization and cytotoxicity studies

Aditya Nath Pandey, Kuldeep Rajpoot, Sunil K. Jain *

Institute of Pharmaceutical Sciences, Guru Ghasidas Vishwavidyalaya (A Central University), Bilaspur (C.G.) 495 009, INDIA

ABSTRACT

Objective(s): Colorectal cancer (CRC) is a prevalent cancer worldwide. The present study aimed to synthesize and investigate the potential of wheat germ agglutinin (WGA) conjugated with polylactic-co-glycolic acid (PLGA) nanoparticles (NPs) incorporating 5-fluorouracil (5-FU).

Materials and Methods: The NPs were investigated in terms of various characteristics, such as the particle size, surface charge, surface morphology, entrapment efficiency rate, and in-vitro drug release profile in simulated gastric and intestinal fluids. The optimized NPs were conjugated with WGA and characterized for the WGA conjugation efficiency, mucoadhesion, and cytotoxicity studies.

Results: The zeta potential of the WGA-conjugated NPs decreased (-17.9±1.4 mV) possibly due to the conjugation of the NPs with WGA, which reduced the zeta potential. The WGA-conjugated NPs exhibited sustained drug release effects ($p<0.05$) compared to the marketed formulation containing 5-FU after 24 hours. In addition, the optimized NPs followed the Higuchi kinetics, showing diffusion-controlled drug release mechanisms. Finally, the WGA-conjugated PLGA NPs could significantly inhibit the growth of colon cancer cells (HT-29 and COLO-205) compared to the non-conjugated NPs and pure drug solution ($P<0.05$).

Conclusion: According to the results, the WGA-conjugated NPs could be potential carrier systems compared to the non-conjugated NPs for the effective management of CRC.

Keywords: *Carbodiimide Linking, COLO-205, Nanoparticles, PLGA, Wheat Germ Agglutinin, 5-Fluorouracil*

How to cite this article

Nath Pandey A, Rajpoot K, Jain S K. Using 5-fluorouracil-encored plga nanoparticles for the treatment of colorectal cancer: the in-vitro characterization and cytotoxicity studies. Nanomed J. 2020; 7(3): 211-224. DOI: 10.22038/nmj.2020.07.0005

INTRODUCTION

Colorectal cancer (CRC) is highly prevalent in men and women worldwide, ranked the third and second most common cancer, respectively. Similar to other cancers, the current therapies for CRC are not adequately effective due to the lower efficacy of the drug concentrations at the tumor site [1]. One of the common drugs used for this purpose is 5-fluorouracil (5-FU), which is extensively used as an anticancer agent for the inhibition of thymidylate synthetase to induce apoptosis in cancer cells [2]. However, 5-FU has several limitations, such as short biological half-life [3], erratic oral bioavailability, non-selective biodistribution, and drug resistance in malignant cells [4]. Furthermore, 5-FU has rapid degradation in the body, and high doses of drugs are required for proper efficacy [5, 6]. Therefore, the continuous infusion of the drug is required to overcome these limitations, which in turn leads to patient noncompliance and increased treatment costs [7].

A targeted drug delivery system must be applied to deliver the drug more effectively for the management of CRC. Several novel platforms have been proposed in this regard, including microspheres [8, 9], microbeads [10, 11], and nanoparticles (NPs) [12], which have been investigated for the controlled release and targeting effects of drugs in the gastrointestinal (GI) tract. In addition, the poly-lactic-co-glycolic acid (PLGA) polymer has been used for the preparation of NPs in numerous studies not only due to the biocompatible and biodegradable nature of the polymer, but also owing to its potential to control the release of drugs from NPs [13, 14].

* *Corresponding Author Email: suniljain25in@yahoo.com*

Note. This manuscript was submitted on February 5, 2020; approved on March 15, 2020

Numerous investigations have been performed using PLGA-based NPs to enhance the antitumor efficacy of 5-FU against CRC [15-17]. In addition, PLGA NPs incorporating various anticancer agents have been expansively studied for cancer targeting through the attachment of specific ligands; such examples are hyaluronic acid, folic acid, and wheat germ agglutinin (WGA) [18]. The ligand conjugated system may not only increase the residence time of the delivery system at the site of action, but it could also improve the targeting potential of the drug [19-21]. WGA (36 kDa) is a lectin derivative, which is isolated from *Triticum vulgaris* and could selectively bind to the N-acetyl-D-glucosamine and sialic acid residues in the intestinal mucus and glycocalyx of the intestinal enterocytes [22]. In this regard, Yin et al. have reported the potential of WGA-conjugated PLGA NPs for the oral delivery of thymopentin [23].

The present study aimed to formulate a lectin-conjugated NP delivery system using 5-FU for the effective treatment of CRC. To this end, PLGA NPs encapsulated with 5-FU were prepared and conjugated with WGA for controlled, site-specific, and targeted drug delivery.

Materials and Methods

Experimental materials

In this study, 5-FU and WGA were provided by the M/S Avra Synthesis Pvt. Ltd. (Hyderabad, India) and the Bio-research Products Inc. (323 W. Cherry St., North library [IA 5231]), respectively. PLGA (50:50), N-hydroxysuccinimide (NHS), 1-ethyl-3, 3-(dimethyl aminopropyl) carbodiimide (EDC), pluronic F-68, and fluorescein isothiocyanate (FITC) were also purchased from HiMedia Laboratories Pvt. Ltd.

Table 1. Formulation Code, Variables, Particle Size, and Drug Entrapment Rate

S. No	Formulation Code	Drug:Polymer Ratio	Stirring Time (h)	Particle Size (nm)	Drug Entrapment (%)
1	FUNP1	1:1	2	120.0±3.5	82.14±0.84
2	FUNP2	1:1	3	112.0±2.1	82.59±0.73
3	FUNP3	1:1	4	103.0±4.4	85.04±0.93
4	FUNP4	1:2	2	210.7±3.6	83.12±0.82
5	FUNP5	1:2	3	188.4±1.7	82.83±0.60
6	FUNP6	1:2	4	178.3±2.3	84.12±0.52
7	FUNP7	1:3	2	260.0±1.8	76.53±0.64
8	FUNP8	1:3	3	216.3±1.7	75.21±0.63
9	FUNP9	1:3	4	196.0±3.7	75.16±0.83

Mean±SD; n=3; FUNP1-9: NP formulation containing 5-FU as a drug

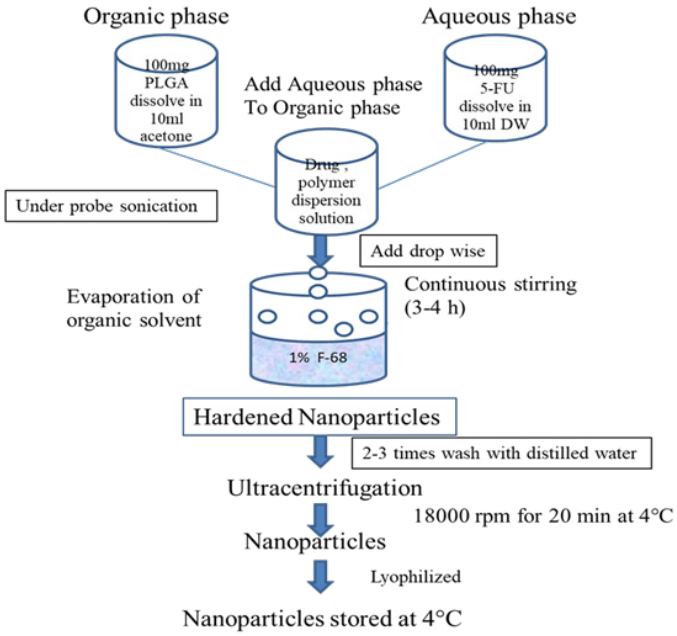

Fig 1. Schematic diagram of NP Preparation

(Mumbai, India). In addition, Eudragit S100 was obtained from the Evonik Degussa Pvt. Ltd. (Mumbai, India). Human colon cancer cells (HT-29) and COLO-205 cells were procured from the National Center for Cell Sciences (NCCS) in Pune, India). The other chemicals and reagents were of the analytical reagent grade.

Preparation of the 5-FU-loaded PLGA NPs

Initially, the 5-FU-loaded PLGA NPs were prepared using the solvent evaporation method with slight modifications [23, 24]. In brief, PLGA was dissolved in acetone at various concentrations (Table 1). A solution of the 5-FU drug was also prepared in distilled water. Afterwards, the 5-FU solution was added to the PLGA solution under probe sonication using the frontline sonicator (Unitech Instruments, Vadodara), and the dispersion was further sonicated for 10 minutes. The resulting dispersion was added in a dropwise manner to 100 milliliters of the pluronic F-68 solution (1% w/v) using a needle (24 G) with constant stirring at room temperature in order to obtain particles of the desired size. Following that, the obtained NPs were washed with distilled water under cooling ultracentrifuge (Remi Cooling Ultracentrifuge; Mumbai, India) at 18,000 rpm for 20 minutes at the temperature of 4°C. Finally, the NPs were lyophilized using the MAC Lyophilizer (Macro Scientific Works Pvt. Ltd., Delhi, India) and stored at the temperature of 4°C. Fig 1 shows the schematic diagram of the NP preparation process.

WGA-conjugation with the NPs

The conjugation of WGA with the PLGA NPs was carried out using the carbodiimide method [25, 26]. The optimized NPs (i.e., FUNP3) were used for WGA conjugation and designated in the form of WFUNP3. In brief, the carboxyl group of the NPs (100 mg) was activated by adding 1-ethyl-3, 3-(dimethylaminopropyl) carbodiimide (EDC, 0.1 M) and N-hydroxysuccinimide (NHS, 0.1 M) to phosphate buffer (pH: 7.4) for three hours at room temperature.

The excess EDC and NHS were removed by washing with phosphate buffer (pH: 7.4), followed by addition to the WGA solution (10 ml) that was prepared in phosphate buffer (pH: 7.4) and incubated overnight.

The WGA-conjugated NPs were separated via centrifugation at 18,000 rpm, followed by washing with distilled water trice. Finally, the obtained WGA-conjugated NPs were lyophilized and stored at the temperature of 4^{o}C.

Coating of a hard gelatin capsule with eudragit S100

A polymer solution of Eudragit S100 (4%) in isopropyl alcohol (50 ml) and PEG-400 (5% w/v) as the plasticizer [27] was used for the coating of the capsules containing WFUNP3 and FUNP3, which were dried in a hot air oven at a moderate temperature (35-45°C).

The coating process of the polymer solution was repeated to achieve the desired level of coating.

Characterization

Infrared spectroscopy

The infrared (IR) spectroscopy of the pure drug, polymer, WGA, and prepared formulations (conjugated/non-conjugated) was performed using a Fourier-transform infrared spectroscopy (FTIR) spectrophotometer (IR Affinity-1, Shimadzu Corp, Japan), and the spectra were scanned within the range of 400-4,000 cm^{-1}.

WGA-conjugation efficiency

The amount of the WGA binding to the PLGA NPs was determined by determining the difference between the added and recovered quantity of WGA after incubation. In addition, the amount of WGA in the supernatant was estimated using the Folin-Ciocalteu reagent. Reagents A and B were prepared by dissolving Na_2CO_3 (2 g) in 0.1 N NaOH and $CuSO_4.5H_2O$ (0.5 g) in 1% sodium/potassium tartrate in order to prepare 100 milliliters of solutions for each, respectively. Reagent C was also prepared by mixing 50 milliliters of reagent A with 1.0 milliliter of reagent B. Finally, reagent D was prepared by diluting Folin-Ciocalteu phenol (2.0 N) with distilled water to achieve 1.0 N.

Reagent C (10 ml) was added to a suspension containing 100 milligrams of the WGA-conjugated NPs in 100 milliliters of distilled water, mixed carefully, and allowed to stand for 30 minutes. Following that, reagent D (2.0 ml) was added to the mentioend solution through instant mixing. After 30 minutes of constant mixing, the solution was filtered under vacuum, with the volume reaching 20 milliliters. Finally, the samples were subjected to absorbance at 750 nanometers against blank using a UV-visible spectrophotometer (Shimadzu 1800, Japan) [27-29].

Shape and surface morphology

The morphology of the optimized and WGA-conjugated formulations was assessed using transmission electron microscopy (TEM). The samples were fixed with 2.0% phosphotungstic acid and examined using a TEM device (Morgagni 268D, Fei Electron Optics, USA) at the Electron Microscopy Division (AIIMS, New Delhi, India).

Particle size, size distribution, and zeta potential

The mean particle size, size distribution, and zeta potential of the optimized 5-FU-loaded and WGA-conjugated NPs were determined using the Malvern Zetasizer (Malvern Instruments Ltd., UK).

Entrapment efficiency of the PLGA NPs

The drug entrapment efficiency of the PLGA NPs was evaluated using an indirect method [30]. In brief, the unentrapped (free) drug was separated through the ultra-centrifugation of the samples at 3,000 rpm for 15 minutes and washing trice. The collected supernatant was analyzed using a UV spectrophotometer (Shimadzu 1800, Japan) at 266 nanometers, and the free drug was determined using the following equation:

$$Entrapment\ Efficiency\ (\%) = \frac{5FU_{total} - 5FU_{free}}{5FU_{total}} \text{X}100$$

Differential scanning calorimetry (DSC)

The samples were analyzed using a differential scanning calorimetry (DSC) instrument (DSC-60, Shimadzu Corp, Japan). To do so, approximately five milligrams of the drug, polymer, and formulations were weighed into an aluminum pan and sealed with a pin-holed lid. Afterwards, the thermogram was recorded in a nitrogen atmosphere within the temperature range of 10-300°C at the heating rate of 10°C per minute. The baseline optimization was performed before each run.

In-vitro Studies

Drug release analysis

The *in-vitro* release of 5-FU from the NPs was carried out in 20 milliliters of the simulated intestinal fluid (SIF; pH: 7.4), which was preserved at the temperature of 37±0.5ºC. The Franz diffusion cells were also used with the effective surface area of 2.06 cm^2 at the rotation speed of 100 rpm. A cellulose acetate membrane (molecular weight cutoff: 5 kDa; size cutoff: 0.22 µm) was inserted between the donor and receptor chambers. Aliquots (1.0 ml) were withdrawn at predetermined intervals and replenished with equal volumes of pre-heated, fresh media to maintain a constant volume. Following that, the sample was diluted, filtered using a Whatman filter paper (#41), and analyzed at 266 nanometers in order to determine the concentration of the drug present in the dissolution medium. Moreover, the *in-vitro* drug release analysis of the WGA-conjugated formulation and powder of the marketed formulation of 5-FU (i.e., chemoflura capsule [250 mg]; Neon Laboratories Ltd., India) was performed following the same procedure. It is notable that the analysis was performed in triplicate.

The 5-FU drug release from the non-conjugated and WGA-conjugated PLGA NPs was statistically analyzed using one-way analysis of variance (ANOVA) with a posttest (Dunnett's multiple comparison test). Additionally, the GraphPad-InStat software (GraphPad-Instat Software Inc., San Diego) was employed for the calculations. The kinetic models of zero-order, first-order, Higuchi, Peppas-Korsmeyer, and Hixson-Crowell release equations were applied to process the *in-vitro* release data and determine the equation with the best fit using the Microsoft Excel software package version 2010.

Simulated GI fluid

The Eudragit S100-coated gelatin capsules were placed in a basket containing the dissolution medium (900 ml), the temperature of which was thermostatically controlled at 37±0.5 ºC, and the rotation speed of the basket was 100 rpm. Initially, the pH of the dissolution medium was maintained at 1.2 for two hours as specified in I.P. After two hours, the capsules were transferred to the buffer medium (pH: 4.5) and maintained for two hours. After four hours, the pH of the medium was adjusted to 7.4 and maintained for 24 hours [31, 32]. The samples were withdrawn from the dissolution medium at various intervals using a pipette, replaced with fresh phosphate buffer with the pH of 1.2, 4.5, and 7.4, and analyzed using a UV-Vis spectrophotometer at 266 nanometers.

Colonic fluid (2.0% Rat Cecal Content)

The *in-vitro* drug release analysis of the optimized coated formulation was carried out using the basket dissolution apparatus. The capsule was placed in the basket, and the basket was dipped in 900 milliliters of the dissolution medium

(phosphate buffer pH: 6.8) containing 2% (w/v) rat cecal content [31, 32]. The experiment was performed with continuous CO_2 supplementation of the dissolution medium. The samples were withdrawn from the dissolution medium at various intervals using a pipette and replaced with fresh phosphate buffer (pH: 6.8). Afterwards, the samples were withdrawn using a pipette into a series of 10-milliliter volumetric flasks, with the volume determined to mark with phosphate buffer (pH: 6.8), followed by centrifugation. The supernatant was filtered through a Whatman filter paper (#41), and the filtrate was analyzed using the UV-Vis spectrophotometer in terms of the 5-FU content at 266 nanometers.

In-vitro Cytotoxicity Assessment

The cytotoxicity assessment of the 5-FU, FUNP3, and WFUNP3 formulations was conducted using the sulforhodamine B (SRB) assay [33, 34]. In this process, the two cell lines of HT-29 and COLO-205 were cultivated in the RPMI 1640 medium, which comprised of L-glutamine (2 mM) and 10% fetal bovine serum. Afterwards, the cells were inoculated into 96-well microtiter plates (5,000 cells per well).

After the cell inoculation, the microtiter plates were incubated at the temperature of 37°C with 5% CO_2, 95% air, and 100% relative humidity for 24 hours prior to the testing of the NPs (FUNP3 and WFUNP3).

Furthermore, the NP formulation, plain 5-FU, and adriamycin (ADR; positive control) were added to the microtiter wells, which contained 90 microliters of the medium at this stage.

At the next stage, the plates were incubated for 48 hours, and the SRB assay was terminated, and the cells were fixed *in-situ* by the gentle addition of 50 microliters of cold 30% (w/v) trichloroacetic acid (TCA) (10% TCA), followed by incubation for one hour at the temperature of 4°C. The supernatant was discarded, and the plates were washed properly and air-dried. Furthermore, 50 microliters of the SRB solution (0.4% w/v) was prepared in 1.0% acetic acid and added to each well, and the plates were incubated for 20 minutes. All the experiments were carried out at room temperature.

After staining, the unbound dye was recovered, and the residual dye was removed by washing five times with 1.0% acetic acid. Following that, the plates were air-dried, the bound stain was eluted with a trizma base (10 mM), and the absorbance was read using an ELISA plate reader at the wavelength of 540 nanometers (reference wavelength: 690 nm).

Growth rate was calculated on a plate-by-plate basis for the test wells relative to the control wells using the following equation:

$$\%\ Growth = \frac{Average\ Absorbance\ of\ Test\ Well}{Average\ Absorbance\ of Control\ Well} \times 100$$

A dose-response curve was also prepared by depicting various concentrations of 5-FU on the X axis as opposed to the absorbance on the Y axis. Cell viability was measured by calculating the relative absorbance of the treated cells compared to the untreated controlled cells. Cell morphology was also observed using an inverted phase-contrast microscope, and the cell viability rate was calculated using the following equation:

$$\%\ Cell\ Viability = \frac{Abs}{Abc} \times 100$$

where *Abs* is the absorbance of the treated cells, and *Abc* represents the absorbance of the untreated control cells.

In-vivo Studies

Mucoadhesion Analysis

The 5-FU, FUNP3, and WFUNP3 formulations were added separately to 1.0 milliliter of an ethanol solution containing 1.0% (w/v) FITC and incubated for 24 hours prior to the mucoadhesive analysis [28]. In addition, a mucoadhesive study of Wistar rats (weight: 220±20 g) was conducted in accordance with the guidelines, in which the rats were kept fasting overnight with *ad libitum* access to water. Afterwards, the animals were sacrificed, and their fresh colon was collected. The colonic contents found in the collected colons were removed by rinsing with warm Tyrode's solution (37°C).

Following that, the colonic part was divided into four equal segments, and three segments were dipped into a suspension containing 10 milligrams of each fluorescent formulation (5-FU in 5 ml of SIF; pH: 7.4), and the control segment was dipped in the fluorescent marker only. All the segments were immediately incubated in the dark in the Tyrode's solution gassed with oxygen at the temperature of 37°C [35]. After two hours, the colonic segments were washed thrice in ice-cold SIF in order to remove the residual NPs and observed using a fluorescent microscope (Carl Zeiss, Germany).

RESULTS AND DISCUSSION

Preparation of the PLGA NPs

In general, the size of the NPs depends on the size of the droplets and stability of the emulsion. When mixed in the external phase, pluronic F-68 (a nonionic surfactant) stabilizes the emulsion, thereby facilitating the formation of small droplets. In a previous study, PLGA NPs coated with pluronic F-68 asnon-digestible synthetic polymers were reported to act as potential carrier systems for oral administrations [36]. Pluronic F-68 is a swellable, hydrophilic polymer, and the higher content of residual pluronic F-68 on the surface of PLGA NPs may indicated their hydrophilicity [37]. In the present study, a large amount of pluronic F-68 coating around the PLGA NPs could form a hydrogel barrier to control the diffusion release of 5-FU from the PLGA NPs. It is notable that the solidification of the NPs was due to the slow evaporation of acetone at room temperature.

The NPs were optimized by formulating various batches of the NPs at different stirring times (2, 3 and 4 hours) and drug-to-polymer ratios of 1:1, 1:2, and 1:3. The obtained results suggested that the particle size increased with the increased polymer content and constant amount of the drug and stirring speed, which could be attributed to the accumulation or layering of the polymer on the particle surface [23, 38]. On the other hand, the particle size decreased with the increased stirring time, which could be due to the friction between the particles and inner wall of the beaker, as well as the friction among the particles.

Conjugation of WGA with the NPs

In the current research, the carbodiimide technique proposed by Mo and Lim [39, 40] was employed for the conjugation of the optimized PLGA NPs (i.e., FUNP3). In this method, carbodiimide or glutaraldehyde was used as the coupling agent [29]. In the case of PLGA, the groups present on the surface (e.g., hydroxyl or carboxyl) could be functionalized using targeting moieties. Moreover, these functional groups were likely to be masked due to the presence of surface additives [35].

EDC reacts with a carboxyl group of PLGA, thereby forming an amine-reactive O-acylisourea intermediate. This intermediate may have a high affinity to react with an amine group of WGA to produce a conjugate [28]. Furthermore, the addition of NHS could stabilize the amine-reactive intermediate through its conversion into an amine-reactive NHS ester, which increased the efficiency of the EDC-mediated coupling reactions [41, 42].

As a result, the amine-reactive NHS ester intermediate had sufficient stability to allow two-step cross-linking procedures, which allowed the conjugation of carboxyl groups of PLGA with the amine group of WGA [43]. In the conventional carbodiimide method, considerable amounts of the drug were released into the external aqueous medium during the incubation of WGA with the PLGA NPs, while also partially reacting with the carboxylated PLGA.

This reaction significantly reduced the drug loading efficiency and yield of lectin conjugation.

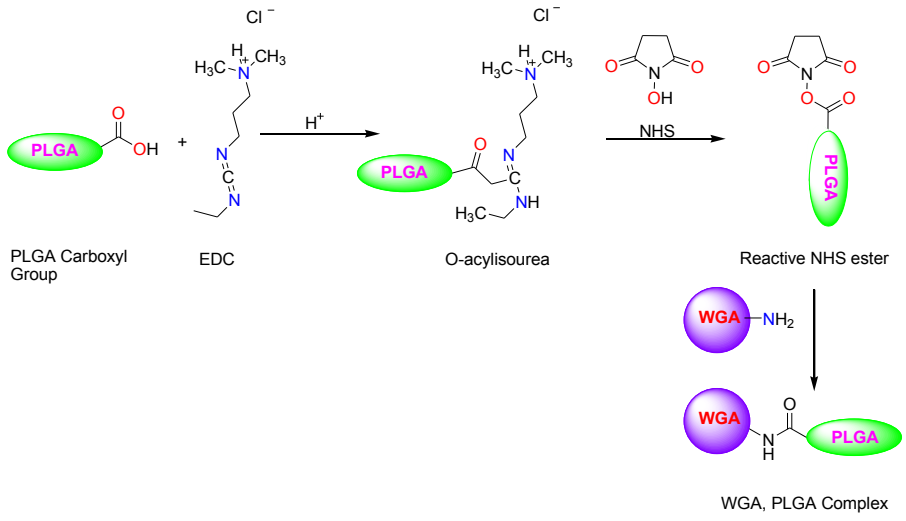

Fig 2. Reaction Scheme of WGA Conjugation with PLGA NPs Using Stable Amide Bond Formation

Therefore, we developed a novel method for the surface engineering of the PLGA NPs with WGA. The coupling of WGA with PLGA NPs depends on the formation of the amide bond between the NH_2 groups of WGA and COOH-group of PLGA. After conjugation in the present study, the conjugation rate of WFUNP3 was estimated at 81.58±0.052%. Fig 2 depicts the reaction scheme of WGA conjugation with the PLGA NPs through the stable amide bond formation.

Characterization of the NPs

Infrared spectroscopy

Fig 3 shows the FTIR spectra of the pure 5-FU, PLGA, WGA, 5-FU-loaded FUNP3 (non-conjugated PLGA NPs), and WFUNP3 (WGA-conjugated PLGA NPs).

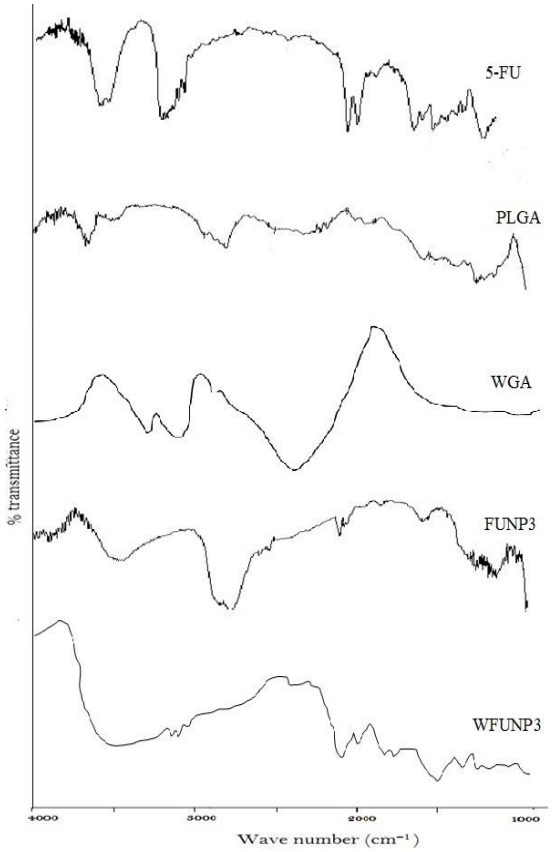

Fig 3. Infrared Spectra of 5-FU, PLGA, WGA, FUNP3, and WFUNP3

The IR spectrum of 5-FU showed the characteristic peaks at 3,212.40, 1,712.79, 1,643.35, 1,249.87, and 1,180.44 cm^{-1} in various functional groups, including the N-H stretch, C=O stretch, C-N stretch, C-H, and C-O stretch, respectively. In addition, the obtained IR spectrum of PLGA showed various peaks at 2,936, 1,711, and 1,314 cm^{-1} for the C-H stretch, carbonyl (ketone) group, and ether, respectively. As for the non-conjugated NPs (FUNP3), the peaks were obtained at 3,147.83, 1,720.50, 1,658.78, and 1,249.87 cm^{-1} for various functional groups, including the N-H stretch, C=O stretch, C-N stretch, and C-H stretch, respectively.

In the case of WGA, the IR spectrum indicated the characteristic peaks at 3,300 cm^{-1} for the N-H stretch, as well as at 1,629.4 and 1,510.3 cm^{-1} for the amine group. However, the peaks observed for the amide groups in WFUNP3 (3,398.97, 1,764.87, 1,631.78, and 1,452.40 cm^{-1}) revealed the presence of the amide bond in the formulation. Furthermore, the amide bonds were confirmed by the presence of two peaks at 1,631.78 and 1,452.40 cm^{-1}, which are the characteristics of amides mainly in proteins.

Shape and surface morphology

The surface morphology and shape of the non-conjugated NPs (FUNP3) and WGA-conjugated NPs (WFUNP3) were analyzed using TEM at various magnifications. The photomicrograph indicated that the particles were uniform in terms of the size and spherical in terms of the shape (Fig 4).

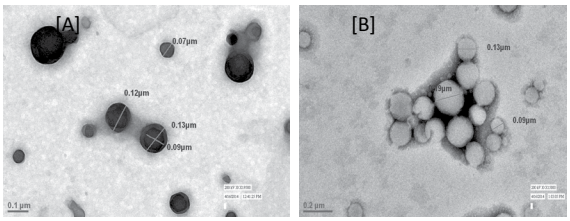

Fig 4. TEM Photomicrograph of Optimized Formulations: A) FUNP3 and B) WGA-conjugated WFUNP3

Moreover, the size of the conjugated NPs slightly increased, which could be attributed to the conjugation of lectin on the surface of the NPs compared to the non-conjugated NPs.

Particle size, size distribution, and zeta potential

The mean particles size of the 5-FU-loaded NPs with the selected drug-to-polymer ratios of 1:1, 1:2, and 1:3 was estimated at 103.0±4.4-120.4±3.5, 178.3±2.3-210.7±3.6, and 196.0±3.7-260.0±1.8 nanometers, respectively (Table 1). Therefore, it could be inferred that the mean particle size of the NPs was directly correlated with the PLGA concentration. The dataset for the

stirring time of various batches indicated that the increased stirring time was associated with the decreased particle size. Furthermore, the particles with smaller sizes were produced with lower polymer concentration in proportion to the higher surface area per unit volume. These findings are consistent with the results obtained by Araujo et al. [44], which showed the size of WGA-conjugated NPs (WFUNP3) to be 155.6±2.5 nanometers. The mentioned findings also demonstrated that the conjugation of the NPs with WGA increased the particle size ($P<0.05$).

Before WGA conjugation, the zeta potential of the NPs was -26.7±1.2 mV, indicating that the surface of the NPs was negatively charged. After the WGA binding, the decreased zeta potential (-17.9±1.4 mV) showed that the changes in the particle charge of the NPs were due to WGA conjugation.

The negative surface charge of the 5-FU NPs might be due to the presence of the uncapped carboxylic groups of the polymers on the NP surfaces. In a study in this regard, Bogataj et al. reported the reduced negative value of the zeta potential also decreased repulsion, which in turn increased the mucoadhesion strength of NPs [45]. In another research, WGA was reported to bear a positive charge at neutral pH, which might contribute to the reduction of the zeta potential of negatively charged lipid NPs following WGA conjugation [46].

Entrapment efficiency of the PLGA NPs

According to the findings of the current research, the entrapment efficiency rate of the NPs was 75.16±0.83-85.04±0.84% (Table 1). The variation in the entrapment efficiency could be due to the changes in the particle size and decreased polymers to encapsulate the drug. Furthermore, FUNP3 showed the optimal results in terms of entrapment efficiency (85.04±0.84%) and particle size (103.0±4.4 nm).

The drug entrapment efficiency of the NPs was substantially influenced by the concentration of the polymer and surfactants [7] as the increased concentration of the polymer was associated with the lower entrapment efficiency of the drug in the WGA-modified NPs.

This could be attributed to the increased viscosity of the dispersed phase, which negatively affected the drug entrapment efficiency of the NPs [47].

DSC analysis

The melting peak of 5-FU was observed at 284.02ºC, indicating the crystalline form of 5-FU [48]. In addition, the PLGA and 5-FU-loaded NPs indicated an endothermic peak at 58.18ºC and 59.96ºC, respectively (Fig 5).

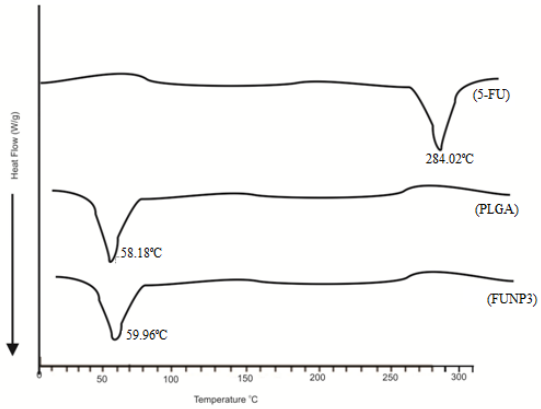

Fig 5. DSC Thermogram of 5-FU, PLGA, and Optimized NPs (FUNP3)

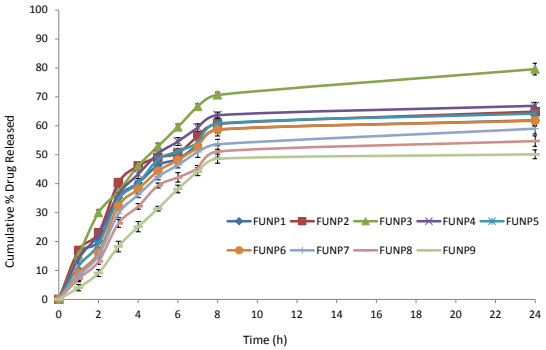

Fig 6. In-vitro Drug Release Profile of 5-FU in Various Formulation Batches in SIF (pH: 7.4; values expressed as mean±SD; n=3)

However, 5-FU showed no characteristic peak in the drug-loaded PLGA NPs. The reduced height and sharpness of the endotherm peak might be due to the loss of the crystalline property of the PLGA polymer in the NPs, which is in line with the results obtained by Mu and Feng. In the current research, no detectable endothermic peak was recorded for the drug, while the drug was present in the formulation in the amorphous form [49].

In-vitro Studies

Drug release analysis

The *in-vitro* drug release of 5-FU was observed in an increasing order from drug-to-polymer ratios of 1:3 (FUNP7, FUNP8, and FUNP9), 1:2 (FUNP4, FUNP5, and FUNP6), and 1:1 (FUNP1, FUNP2, and FUNP3) (Fig 6).

Table 2. Results of One-way ANOVA and Dunnett's Multiple Comparisons Test for In-vitro Release of Optimized Formulation of 5-FU in SIF

Comparison	Mean Difference	q	P-value
Control (MF) vs. FUNP3	29.362	2.866*	<0.05
Control (MF) vs. WFUNP3	31.529	3.078*	<0.05

Moreover, the decreased drug release from the formulation might be due to the higher polymer concentration, which in turn resulted in the formation of a denser polymer network of the formulation, hindering drug release [28].

According to the results of the present study, the particle size markedly influenced drug release as evidenced by the release pattern. The particles with smaller sizes showed the maximum drug release, which might be due to the higher exposure of the particle surfaces to the biological environment. The increased exposure allows the higher penetration of water into the polymeric matrix, thereby facilitating the diffusion process of the drug from NPs [50]. Slow drug release could be caused by the diffusion of the drug from the NP matrix following polymer degradation.

The findings of the current research regarding the rate of the cumulative drug release curve from chemoflura indicated that 75.82% of 5-FU was released after four hours, while in the FUNP3 and WFUNP3 formulations, the rate was estimated at 48.12%, and 42.32% after four hours, respectively (Fig 7).

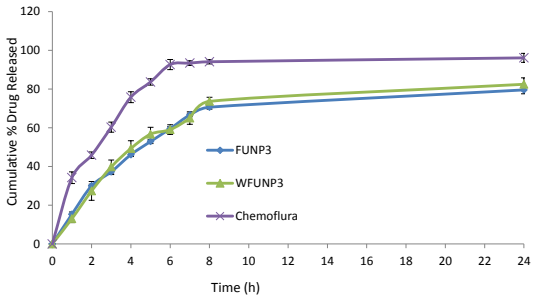

Fig 7. Comparative In-vitro Drug Release Profile of 5-FU from Non-conjugated NPs (FUNP3), WGA-conjugated NPs, and Marketed Formulations (Chemoflura) (Values expressed as mean±SD; n=3)

The conjugated NPs showed a sustained drug release profile within 24 hours compared to the marketed formulation containing 5-FU (P<0.01). On the other hand, WGA conjugation had no significant impact on the integrity of the NPs and only slightly decreased the *in-vitro* release of 5-FU, thereby encouraging the sustained release of the drug.

In the present study, WFUNP3 showed the cumulative drug release rate of 82.48±3.32% compared to FUNP3 (79.51±2.03%) after 24 hours. However, the drug release pattern of WFUNP3 exhibited an insignificant effect compared to FUNP3 (P>0.05), while the WGA conjugation to the NPs revealed reduced the drug release compared to the non-conjugated formulations. These findings are in congruence with a study in which folic acid-conjugated NPs could decrease drug release as opposed to non-conjugated NPs [19, 20].

In the current research, the data obtained from the *in-vitro* release analysis of the marketed formulation of the 5-FU capsule (chemoflura [250 mg], Neon Laboratories Ltd., India) were compared with the *in-vitro* release profile of the optimized non-conjugated (FUNP3) and conjugated formulations (WFUNP3) in the SIF with the pH of 7.4 using one-way ANOVA and Dunnett's multiple comparison test. According to the findings, the *in-vitro* 5-FU release from FUNP3 and WFUNP3 was significantly different compared to the release profile of chemoflura (P<0.05) (Table 2).

In the present study, both the conjugated and non-conjugated formulations were subjected to various kinetic models (zero-order, first-order, Higuchi kinetics, Korsmeyer-Peppas kinetics, and Hixson Crowell) in order to determine the type of the diffusion involved in the drug release from the NPs. The first-order kinetics was observed for 5-FU based on the release data of various NPs (i.e., FUNP1, FUNP4, FUNP5, FUNP6, FUNP7, and FUNP8). On the other hand, the FUNP9 formulation showed zero-order kinetics, and the release kinetics of 5-FU in the FUNP2 and FUNP3 formulations complied with the Higuchi kinetics as confirmed by the maximum R^2 values. In addition, the release of the 5-FU molecule from the optimized formulations followed the Higuchi kinetics based on the polymer matrix [51], which specifically released the drug through the diffusion-controlled mechanism [52, 53].

As expected, the formulations revealed a particle size-dependent drug release pattern in the current research. Correspondingly, the

Table 3. Release Kinetics of Various NPs Containing 5-FU

Formulation Code	Correlation-coefficient (R^2)					
	Zero-order	First-order	Higuchi Kinetics	Korsmeyer-Peppas	Hixson-Crowell	Best Fit Model
FUNP1	0.942	0.980	0.976	0.965 (n=0.449)	0.970	First
FUNP2	0.907	0.958	0.973	0.953 (n=0.422)	0.943	Higuchi
FUNP3	0.965	0.997	0.998	0.99 (n=0.545)	0.996	Higuchi
FUNP4	0.956	0.992	0.975	0.985 (n=0.505)	0.984	First
FUNP5	0.953	0.984	0.961	0.973 (n=0.577)	0.976	First
FUNP6	0.962	0.988	0.950	0.969 (n=0.678)	0.982	First
FUNP7	0.959	0.984	0.948	0.970 (n=0.715)	0.978	First
FUNP8	0.967	0.986	0.942	0.973 (n=0.769)	0.981	First
FUNP9	0.994	0.990	0.897	0.911 (n=1.115)	0.993	Zero
WFUNP3	0.956	0.989	0.971	0.977 (n=0.542)	0.986	First
MF	0.888	0.974	0.984	0.975 (n=0.301)	0.972	Higuchi

FUNP1-9 : NP formulation containing 5-FU as a drug; WFUNP3: WGA-conjugated NPs; MF: marketed formulation of 5-FU

particles with smaller sizes showed greater drug release, which might be attributed to the higher exposure of the particle surfaces to the biological environment. The increased exposure also allowed higher water inclusion within the polymeric matrix network, thereby facilitating the higher diffusion of the drug from the NPs [28, 54]. Moreover, the WGA-conjugated NPs complied with the first-order release kinetics for 5-FU, while the marketed formulation confirmed the Higuchi kinetics (Table 3). In the present study, the drug release from various Eudragit S100-coated capsules enclosing FUNP3 and WFUNP3 was assessed in various pH medium (1.2, 4.5, and 7.4) at the temperature of 37±0.5ºC. The observed drug release pattern from the capsules clearly suggested that the drug was not released for up to two hours (pH: 1.2), while within 2-4 hours (pH: 4.5), the drug was only slightly released (P>0.05). After 24 hours (pH: 7.4), the drug release from FUNP3 and WFUNP3 was estimated at 78.56±3.32% and 77.65±4.32%, respectively (Fig 8).

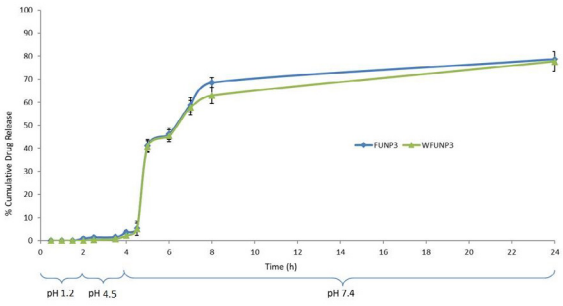

Fig 8. Cumulative Drug Release (%) of Non-conjugated NPs (FUNP3) and WGA-conjugated NPs (WFUNP3) in Simulated GI Fluids (Values expressed as mean±SD; n=3)

As the acrylic polymer was used for the coating of the capsules containing the NPs, which was generally insoluble at acidic pH and dissolved only in the basic environment (pH>7.0), the subjected NPs exhibited no significant drug release in the pH medium of 1.2 and 4.5, while drug release was observed at the pH of 7.4, which could be attrbiuetd to the diffusion and erosion mechanisms [9, 27].

In the current research, the *in-vitro* drug release analysis was performed in the SCF (pH: 6.8) containing 2% rat cecal content for FUNP3 and WFUNP3, and the findings suggested a slight change in the drug release (P>0.05). The reduced release of 5-FU was also observed in the SCF containing 2% rat cecal content, which could be attributed to the increased viscosity of the medium due to the presence of the rat cecal content (Fig 9).

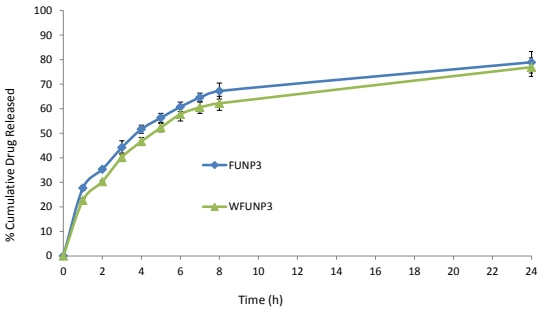

Fig 9. Cumulative Drug Release (%) in SCF (pH: 6.8) Containing 2% Rat Cecal Content of Non-conjugated NPs (FUNP3) and WGA-conjugated NPs (WFUNP3) (Values expressed as mean±SD; n=3)

Cytotoxicity assay

Cell growth inhibition was assessed for 48 hours using the two cell lines of HT-29 and COLO-205 after treatment with various formulations. The concentration of the drugs remained unchanged in both the non-conjugated and conjugated formulations, as well as the free drug solution. The obtained results clearly indicated dose-dependent cytotoxicity as the cell viability rate decreased

with the increased 5-FU concentration. Fig 10 depicts the cell viability of the non-conjugated NPs (FUNP3), WGA-conjugated NPs (WFUNP3), and ADR (control) after treatment with plain 5-FU at various concentrations.

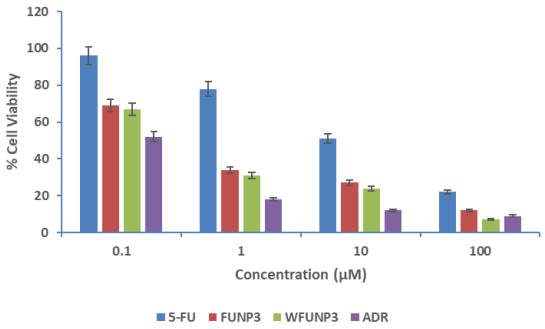

Fig 10. Cell Viability (%) of HT-29 Cells Treated with Free 5-FU Solution, Non-conjugated NPs (FUNP3), WGA-conjugated NPs (WFUNP3), ADR (control), and HT-29 Control after Incubation for 48 Hours (Values expressed as mean±SD; n=3)

Moreover, the cell viability rate of the HT-29 cell line was determined for 5-FU within the concentration range of 0.10-100 µM, and the findings suggested the maximum cell viability rate in the free 5-FU (24.2-94.6%).

In the case of FUNP3, the rate was observed to be lower in the free 5-FU solution (13.4-70.2%), while it was higher in WFUNP3 (6.6-67.4%). As for the COLO-205 cells, the cell viability rate was determined at a similar concentration of 5-FU (0.10-100 µM), and the obtained results revealed the maximum cell viability rate in the free 5-FU (34.2-96.6%).

In the case of FUNP3, the rate was observed to be lower in the free 5-FU solution (23.2-74.4%), while it was higher in WFUNP3 (16.6-70.4%) (Fig 11).

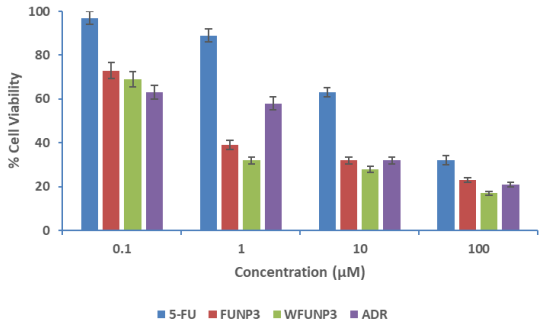

Fig 11. Cell Viability (%) of COLO-205 Cells Treated with Free 5-FU Solution, Non-conjugated NPs (FUNP3), WGA-conjugated NPs (WFUNP3), ADR (control), and COLO-205 Control after Incubation for 48 Hours (Values expressed as mean±SD; n=3)

The findings of the current research indicated the enhanced anticancer activity (6.6% cell viability) against the HT-29 cells in the WGA-conjugated NPs (WFUNP3) after 48 hours. The IC_{50} values of the WFUNP3, FUNP3, and 5-FU solutions were estimated at 1.59, 1.77, and 3.02 µM, respectively. Similarly, the anticancer activity improved in the case of the COLO-205 cells (16.6% cell viability) after 48 hours in WFUNP3. The IC_{50} values of the WFUNP3, FUNP3, and 5-FU solutions were 0.59, 2.68, and 66.79 µM, respectively. The lower cytotoxicity of the free 5-FU could be attributed to the drug resistance, resulting in the efflux of the 5-FU molecules by the P-glycoprotein pumps [55].

Our findings are consistent with two similar studies using 5-FU. Garg et al. reported the cell inhibitory effect of the 5-FU-loaded hyaluronic acid-decorated NPs and the decreased growth inhibition rate of the A549 cells with the increased concentration of 5-FU (10-80 µg/ml) [56]. In another investigation, El-Hammadi et al. reported the cytotoxic effects of a free 5-FU solution and 5-FU-loaded folic acid-grafted NPs against the HT-29 and MCF-7 cells, while also confirming the reduced cell growth with the increased concentration of the drug [4]. Finally, our findings indicated that the WGA-conjugated NPs enhanced the cytotoxicity of 5-FU compared to the pure 5-FU after 48 hours.

In-vivo Studies

Mucoadhesive analysis

Prior to the investigation, it was assumed that WGA could identify the sugar residues (i.e., N-acetylglucosamine and sialic acid) that are often present in the colonic mucosa and bind to competing sugar [57]. As expected, the interaction between the WGA and sugar residues in the epithelial tissues encouraged the bioadhesion of the WGA-conjugated NPs to the intestinal mucosa [58]. However, WGA has been reported to show substantial binding efficiency to human originated intestinal cell lines, human colonocytes, and prostate cancer cells [22]. In this regard, our findings suggested the specific binding of WFUNP3 to the colonic mucosa, while insignificant or no interaction was observed in FUNP3 as evidenced by the fluorescence microscopy (Fig 12). The encouraged bioadhesive property of WFUNP3 might be ascribed to the conjugation of WGA to the NPs [26]. It is also likely that the specific

interactions observed with the WGA-conjugated NPs were due to differences in the glycoconjugate expressions either in the local mucus glycoproteins or the surface of the M cells. Moreover, the use of WGA lectins may increase the intestinal residence time of NP drug delivery systems either at the absorption site or through the action of a drug, thereby improving the bioavailability and efficacy of the drug [59].

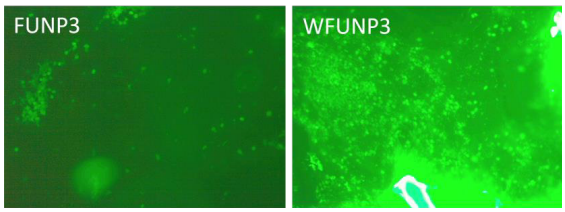

Fig 12. Mucoadhesive Fluorescence Images of Colonic Mucosa Treated with Non-conjugated (FUNP3) and WGA-conjugated NPs (WFUNP3)

CONCLUSION

In the present study, we could successfully develop 5-FU-loaded WGA-conjugated PLGA NPs (WFUNP3) using the solvent evaporation method. According to the results, WFUNP3 exerted sustained drug release effects during 24 hours compared to the marketed formulation of 5-FU (chemoflura) ($P<0.05$). In addition, WFUNP3 had significant inhibitory effects against the two cell lines of HT-29 and COLO-205 compared to the non-conjugated NPs (FUNP3) and drug solutions. WFUNP3 could also enhance the anticancer activity as confirmed by the determined cell viability using the HT-29 (6.6%) and COLO-205 cells (16.6%) after 48 hours. Finally, the *in-vitro* results confirmed that WFUNP3 could be used as a more efficient carrier system for targeted drug delivery in the treatment of CRC compared to FUNP3.

ACKNOWLEDGMENTS

The author Aditya Nath Pandey appreciated the contributions of the ICMR in New Delhi for their financial assistance in the form of SRF (45/74/2012-PHA-BMS).

REFERENCES

1.Siegel RL, Miller KD, and Jemal A. Cancer Statistics, 2017. CA Cancer J Clin 2017;67:7-30.
2.Longley DB, Harkin DP, and Johnston PG. 5-fluorouracil: mechanisms of action and clinical strategies. Nat Rev Cancer 2003;3:330-338.
3.Diasio RB, and Harris BE. Clinical pharmacology of 5-fluorouracil. Clin Pharmacokinet 1989;16:215-237.
4.El-Hammadi MM, Delgado AV, Melguizo C, Prados JC, and Arias JL. Folic acid-decorated and PEGylated PLGA nanoparticles for improving the antitumour activity of 5-fluorouracil. Int J Pharm 2017;516:61-70.
5.van Kuilenburg AB, and Maring JG. Evaluation of 5-fluorouracil pharmacokinetic models and therapeutic drug monitoring in cancer patients. Pharmacogenomics 2013;14:799-811.
6.Mattos AC, Altmeyer C, Tominaga TT, Khalil NM, and Mainardes RM. Polymeric nanoparticles for oral delivery of 5-fluorouracil: Formulation optimization, cytotoxicity assay and pre-clinical pharmacokinetics study. Eur J Pharm Sci 2016;84:83-91.
7.Garg A, Patel V, Sharma R, Jain A, and Yadav AK. Heparin-appended polycaprolactone core/corona nanoparticles for site specific delivery of 5-fluorouracil. Artif Cells Nanomed Biotechnol 2017;45:1-10.
8.Jain SK, Patel K, Rajpoot K, and Jain A. Development of a Berberine Loaded Multifunctional Design for the Treatment of Helicobacter pylori Induced Gastric Ulcer. Drug Deliv Lett 2019;9:50-57.
9.Patrey NK, Rajpoot K, Jain AK, and Jain SK. Diltiazem loaded floating microspheres of Ethylcellulose and Eudragit for gastric delivery: in vitro evaluation. AJBR 2016;2:71-77.
10.Jain SK, Kumar A, Kumar A, Pandey AN, and Rajpoot K. Development and in vitro characterization of a multiparticulate delivery system for acyclovir-resinate complex. Artif Cells Nanomed Biotechnol 2016;44:1266-1275.
11.Jain SK, Prajapati N, Rajpoot K, and Kumar A. A novel sustained release drug-resin complex-based microbeads of ciprofloxacin HCl. Artif Cells Nanomed Biotechnol 2016;44:1891-1900.
12.Rajpoot K. Solid Lipid Nanoparticles: A Promising Nanomaterial in Drug Delivery. Curr Pharm Des 2019;25:1-16.
13.El-Hammadi MM, and Arias JL. Advanced Engineering Approaches in the Development of PLGA-Based Nanomedicines. In Handbook of Nanoparticles: Springer International Publishing, 2016, 1009-1039.
14.Figueiredo M, and Esenaliev R. PLGA Nanoparticles for Ultrasound-Mediated Gene Delivery to Solid Tumors. J Drug Deliv 2012;2012:767839.
15.Shakeri-Zadeh A, Khoee S, Shiran M-B, Sharifi AM, and Khoei S. Synergistic effects of magnetic drug targeting using a newly developed nanocapsule and tumor irradiation by ultrasound on CT26 tumors in BALB/c mice. J Mater Chem B 2015;3:1879-1887.
16.Tang Q, Wang Y, Huang R, You Q, Wang G, Chen Y, Jiang Z, Liu Z, Yu L, Muhammad S, and Wang X. Preparation of anti-tumor nanoparticle and its inhibition to peritoneal dissemination of colon cancer. PLoS One 2014;9:e98455.
17.Wang Y, Li P, Chen L, Gao W, Zeng F, and Kong LX. Targeted delivery of 5-fluorouracil to HT-29 cells using high efficient folic acid-conjugated nanoparticles. Drug Deliv 2015;22:191-198.
18.Badran MM, Mady MM, Ghannam MM, and Shakeel F. Preparation and characterization of polymeric nanoparticles surface modified with chitosan for target treatment of colorectal cancer. Int J Biol Macromol 2017;95:643-649.
19.Rajpoot K, and Jain SK. Colorectal cancer-targeted delivery of oxaliplatin via folic acid-grafted solid lipid nanoparticles: preparation, optimization, and in vitro evaluation. Artif Cells Nanomed Biotechnol 2018;46:1236-1247.

20.Rajpoot K, and Jain SK. Irinotecan hydrochloride trihydrate loaded folic acid-tailored solid lipid nanoparticles for targeting colorectal cancer: development, characterization, and in vitro cytotoxicity study using HT-29 cells. J Microencapsul 2019;36:659-676.
21.Rajpoot K, and Jain SK. Oral delivery of pH-responsive alginate microbeads incorporating folic acid-grafted solid lipid nanoparticles exhibits enhanced targeting effect against colorectal cancer: A dual-targeted approach. Int J Biol Macromol 2020. [Online ahead of print] DOI: 10.1016/j.ijbiomac.2020.02.132
22.Gabor F, Schwarzbauer A, and Wirth M. Lectin-mediated drug delivery: binding and uptake of BSA-WGA conjugates using the Caco-2 model. Int J Pharm 2002;237:227-239.
23.Yin Y, Chen D, Qiao M, Lu Z, and Hu H. Preparation and evaluation of lectin-conjugated PLGA nanoparticles for oral delivery of thymopentin. J Control Release 2006;116:337-345.
24.Zou W, Liu C, Chen Z, and Zhang N. Studies on bioadhesive PLGA nanoparticles: A promising gene delivery system for efficient gene therapy to lung cancer. Int J Pharm 2009;370:187-195.
25.Olde Damink LHH, Dijkstra PJ, van Luyn MJA, van Wachem PB, Nieuwenhuis P, and Feijen J. Cross-linking of dermal sheep collagen using a water-soluble carbodiimide. Biomaterials 1996;17:765-773.
26.Ponchel G, and Irache J. Specific and non-specific bioadhesive particulate systems for oral delivery to the gastrointestinal tract. Adv Drug Deliv Rev 1998;34:191-219.
27.Anande NM, Jain SK, and Jain NK. Con-A conjugated mucoadhesive microspheres for the colonic delivery of diloxanide furoate. Int J Pharm 2008;359:182-189.
28.Jain SK, Haider T, Kumar A, and Jain A. Lectin-Conjugated Clarithromycin and Acetohydroxamic Acid-Loaded PLGA Nanoparticles: a Novel Approach for Effective Treatment of H. pylori. AAPS PharmSciTech 2016;17:1131-1140.
29.Montisci MJ, Giovannuci G, Duchene D, and Ponchel G. Covalent coupling of asparagus pea and tomato lectins to poly(lactide) microspheres. Int J Pharm 2001;215:153-161.
30.Kim JS, Cho KJ, Tran TH, Nurunnabi M, Moon TH, Hong SM, and Lee YK. In vivo NIR imaging with CdTe/CdSe quantum dots entrapped in PLGA nanospheres. J Colloid Interface Sci 2011;353:363-371.
31.Paharia A, Yadav AK, Rai G, Jain SK, Pancholi SS, and Agrawal GP. Eudragit-coated pectin microspheres of 5-fluorouracil for colon targeting. AAPS PharmSciTech 2007;8:12.
32.Rai G, Jain SK, Agrawal S, Bhadra S, Pancholi SS, and Agrawal GP. Chitosan hydrochloride based microspheres of albendazole for colonic drug delivery. Pharmazie 2005;60:131-134.
33.Subudhi MB, Jain A, Jain A, Hurkat P, Shilpi S, Gulbake A, and Jain SK. Eudragit S100 Coated Citrus Pectin Nanoparticles for Colon Targeting of 5-Fluorouracil. Materials (Basel) 2015;8:832-849.
34.Vichai V, and Kirtikara K. Sulforhodamine B colorimetric assay for cytotoxicity screening. Nat Protoc 2006;1:1112-1116.
35.Yin Y, Chen D, Qiao M, Wei X, and Hu H. Lectin-conjugated PLGA nanoparticles loaded with thymopentin: ex vivo bioadhesion and in vivo biodistribution. J Control Release 2007;123:27-38.
36.Hariharan S, Bhardwaj V, Bala I, Sitterberg J, Bakowsky U, and Ravi Kumar MN. Design of estradiol loaded PLGA nanoparticulate formulations: a potential oral delivery system for hormone therapy. Pharm Res 2006;23:184-195.
37.Shenoy DB, and Amiji MM. Poly(ethylene oxide)-modified poly(epsilon-caprolactone) nanoparticles for targeted delivery of tamoxifen in breast cancer. Int J Pharm 2005;293:261-270.
38.Li X, Xu Y, Chen G, Wei P, and Ping Q. PLGA nanoparticles for the oral delivery of 5-Fluorouracil using high pressure homogenization-emulsification as the preparation method and in vitro/in vivo studies. Drug Dev Ind Pharm 2008;34:107-115.
39.Mo Y, and Lim LY. Preparation and in vitro anticancer activity of wheat germ agglutinin (WGA)-conjugated PLGA nanoparticles loaded with paclitaxel and isopropyl myristate. J Control Release 2005;107:30-42.
40.Mo Y, and Lim LY. Paclitaxel-loaded PLGA nanoparticles: potentiation of anticancer activity by surface conjugation with wheat germ agglutinin. J Control Release 2005;108:244-262.
41.Grabarek Z, and Gergely J. Zero-length crosslinking procedure with the use of active esters. Anal Biochem 1990;185:131-135.
42.Staros JV, Wright RW, and Swingle DM. Enhancement by N-hydroxysulfosuccinimide of water-soluble carbodiimide-mediated coupling reactions. Anal Biochem 1986;156:220-222.
43.Jain SK, Gupta M, Sahoo AK, Pandey AN, and Jain AK. Lectin conjugated gastro-retentive microspheres of amoxicillin for effective treatment of Helicobacter pylori. Curr Sci 2014;106:267-276.
44.Araujo J, Vega E, Lopes C, Egea MA, Garcia ML, and Souto EB. Effect of polymer viscosity on physicochemical properties and ocular tolerance of FB-loaded PLGA nanospheres. Colloids Surf B Biointerfaces 2009;72:48-56.
45.Bogataj M, Vovk T, Kerec M, Dimnik A, Grabnar I, and Mrhar A. The correlation between zeta potential and mucoadhesion strength on pig vesical mucosa. Biol Pharm Bull 2003;26:743-746.
46.Liu Y, Li K, Pan J, Liu B, and Feng SS. Folic acid conjugated nanoparticles of mixed lipid monolayer shell and biodegradable polymer core for targeted delivery of Docetaxel. Biomaterials 2010;31:330-338.
47.Xie J, and Wang CH. Self-assembled biodegradable nanoparticles developed by direct dialysis for the delivery of paclitaxel. Pharm Res 2005;22:2079-2090.
48.Ocal H, Arica-Yegin B, Vural I, Goracinova K, and Calis S. 5-Fluorouracil-loaded PLA/PLGA PEG-PPG-PEG polymeric nanoparticles: formulation, in vitro characterization and cell culture studies. Drug Dev Ind Pharm 2014;40:560-567.
49.Mu L, and Feng SS. Fabrication, characterization and in vitro release of paclitaxel (Taxol®) loaded poly (lactic-co-glycolic acid) microspheres prepared by spray drying technique with lipid/cholesterol emulsifiers. J Control Release 2001;76:239-254.
50.Mohammadi G, Nokhodchi A, Barzegar-Jalali M, Lotfipour F, Adibkia K, Ehyaei N, and Valizadeh H. Physicochemical and anti-bacterial performance characterization of clarithromycin nanoparticles as colloidal drug delivery system. Colloids Surf B Biointerfaces 2011;88:39-44.
51.Siepmann J, and Peppas NA. Higuchi equation: derivation, applications, use and misuse. Int J Pharm 2011;418:6-12.

52.Desai KG, and Park HJ. Encapsulation of vitamin C in tripolyphosphate cross-linked chitosan microspheres by spray drying. J Microencapsul 2005;22:179-192.
53.Venkatraman SS, Jie P, Min F, Freddy BY, and Leong-Huat G. Micelle-like nanoparticles of PLA-PEG-PLA triblock copolymer as chemotherapeutic carrier. Int J Pharm 2005;298:219-232.
54.Kalam MA, Humayun M, Parvez N, Yadav S, Garg A, Amin S, Sultana Y, and Ali A. Release kinetics of modified pharmaceutical dosage forms: a review. Cont J Pharm Sci 2007;1:30-35.
55.Fojo T, and Coley HM. The role of efflux pumps in drug-resistant metastatic breast cancer: new insights and treatment strategies. Clin Breast Cancer 2007;7:749-756.
56.Garg A, Rai G, Lodhi S, Jain AP, and Yadav AK. Hyaluronic acid embedded cellulose acetate phthlate core/shell nanoparticulate carrier of 5-fluorouracil. Int J Biol Macromol 2016;87:449-459.
57.Irache JM, Durrer C, Duchêne D, and Ponchel G. In vitro study of lectin-latex conjugates for specific bioadhesion. J Control Release 1994;31:181-188.
58.Khin MM, Hua JS, Ng HC, Wadstrom T, and Bow H. Agglutination of Helicobacter pylori coccoids by lectins. World J Gastroenterol 2000;6:202-209.
59.Irache JM, Durrer C, Duchene D, and Ponchel G. Bioadhesion of lectin-latex conjugates to rat intestinal mucosa. Pharm Res 1996;13:1716-1719.